Prognostic value of RCA pericoronary adipose tissue CT-attenuation beyond high-risk plaques, plaque volume, and ischemia.

Brief title: Prognostic value of PCAT CT-attenuation.

[1]Pepijn A. van Diemen MD[a]; [1]Michiel J. Bom MD[a]; Roel S. Driessen MD[a]; Stefan P. Schumacher MD[a]; Henk Everaars MD[a]; Ruben W. de Winter MD[a]; Peter M. van de Ven PhD[b]; Moti Freiman PhD[c]; Liran Goshen PhD[c]; Dennis Heijtel PhD[c]; Eran Langzam PhD[c]; James K. Min MD[d]; Jonathon A. Leipsic MD[e]; Pieter G. Raijmakers MD, PhD[f]; Albert C. van Rossum MD, PhD[a]; Ibrahim Danad MD, PhD[a]; Paul Knaapen MD, PhD[a]

[1]Both authors contributed equally to the manuscript.

Departments of Cardiology[a], Epidemiology and Biostatistics[b], and PET research and Nuclear Medicine[f], Amsterdam UMC, Vrije Universiteit Amsterdam, Amsterdam, the Netherlands.

[c]Philips Healthcare, Best, The Netherlands

[d]Institute for Cardiovascular Imaging, Weill-Cornell Medical College, New York-Presbyterian Hospital, New-York, United States of America.

[e]Department of Medicine and Radiology, University of British Columbia, Vancouver, Canada.

Relationships with industry and other entities: Dr. Knaapen has received research grants from HeartFlow. Dr. Min is employee and has an equity interest in Cleerly Inc. and serves on the advisory board of Arineta. Dr. Leipsic has received research grants from GE Healthcare and Edwards Lifesciences and serves as consultant for HeartFlow Inc. and Circle CVI. Dr. Freiman, Dr. Goshen, Dr. Heitel, and Dr. Langzam are employees of Philips Healthcare. All other authors have reported that they have no relationships relevant to the contents of this paper to disclose.

Keywords: pericoronary adipose tissue CT-attenuation, coronary inflammation, coronary computed tomography angiography, myocardial ischemia, coronary artery disease.

Word count: 4998

Address for correspondence:

Paul Knaapen, MD, PhD

Department of Cardiology, Amsterdam UMC, Vrije Universiteit Amsterdam

De Boelelaan 1117, 1081 HV Amsterdam, The Netherlands

Telephone: + 31 20 4442441

Fax: + 31 20 4442446

E-mail: p.knaapen@amsterdamumc.nl

Abstract

Objectives: To assess the prognostic value of pericoronary adipose tissue CT-attenuation (PCATa) beyond quantitative coronary computed tomography angiography (CCTA)-derived plaque volume and positron emission tomography (PET) determined ischemia.

Background: Inflammation plays a crucial role in atherosclerosis. PCATa has been demonstrated to assess coronary specific inflammation and is of prognostic value in patients with suspected coronary artery disease (CAD).

Methods: 539 patients who underwent CCTA and [^{15}O]H_2O PET perfusion imaging because of suspected CAD were included. Imaging assessment included coronary artery calcium score (CACS), presence of obstructive CAD (≥50% stenosis) and high-risk plaques (HRP), total plaque volume (TPV), calcified/noncalcified plaque volume (CPV/NCPV), PCATa, and myocardial ischemia. The endpoint was a composite of death and non-fatal myocardial infarction (MI). Prognostic thresholds were determined for quantitative CCTA variables.

Results: During a median follow-up of 5.0 [interquartile range: 4.7-5.0] years, 33 events occured. CACS >59 Agatston, obstructive CAD, HRPs, TPV >220mm^3, CPV>110mm^3, NCPV >85mm^3, and myocardial ischemia were associated with shorter time to the endpoint with unadujsted hazard ratio's (HR) of 4.17 (95% confidence interval (CI): 1.80-9.64), 4.88 (95% CI: 1.88-12.65), 3.41 (95% CI: 1.72-6.75), 7.91 (95% CI: 3.05-20.49), 5.82 (95% CI: 2.40-14.10), 8.07 (95% CI: 3.33-19.55), and 4.25 (95% CI: 1.84-9.78), respectively ($p<0.05$ for all). RCA PCATa above scanner specific thresholds was associated with worse prognosis (unadjusted HR: 2.84 (95% CI: 1.44-5.63), p=0.003), whereas LAD and Cx PCATa were not related to outcome. RCA PCATa above scanner specific thresholds retained is prognostic value adjusted for imaging variables and clincal chacteristics associated with the endpoint (adjusted HR: 2.45 (95% CI: 1.23-4.93), p=0.011).

Conclusions: Parameters associated with atherosclerotic burden and ischemia were more strongly associated with outcome than RCA PCATa. Nonetheless, RCA PCATa was of prognostic value beyond clinical characteristics, CACS, obstructive CAD, HRPs, TPV, CPV, NCPV, and ischemia.

Condensed abstract

Inflammation plays a crucial role in atherosclerosis. Pericoronary adipose tissue CT-attenuation (PCATa) assessed using coronary computed tomography angiography (CCTA) has been linked to coronary inflammation and patient outcome. In the present study, PCATa of the right coronary artery was of prognostic value beyond CCTA and [^{15}O]H_2O positron emission tomography derived parameters; coronary artery calcium score, presence of obstructive disease (≥50% diameter stenosis) and high-risk plaques, total plaque volume, calcified and non-calcified plaque volume, and myocardial ischemia.

Abbreviations

CACS	Coronary Artery Calcium Score
CCTA	Coronary Computed Tomography Angiography
Cx	Circumflex Artery
HRP	High-risk plaque
LAD	Left Anterior Descending Artery
MI	Myocardial infarction
MBF	Myocardial Blood Flow
NCPV	Non-Calcified Plaque Volume
PCATa	Pericoronary Adipose Tissue CT-Attenuation
PET	Positron Emission Tomography
RCA	Right Coronary Artery
TPV	Total Plaque Volume

Introduction

Traditionally assessment of coronary artery disease (CAD) involves determining the anatomical severity and it's functional significance (1). Non-invasively this can be achieved by combined positron emission tomography (PET) and coronary computed tomography angiography (CCTA) imaging (2). In the present cohort we have previously demonstrated that obstructive CAD, high-risk plaques (HRP), and ischemia are associated with outcome, of which obstructive CAD and HRPs were of independent prognostic value (2). However, these markers of CAD do not harbor information regarding the inflammatory burden of a patient. Inflammation plays a crucial role in atherosclerosis, as such accurate assessment of inflammatory risk might improve risk stratification and allow patient tailored anti-inflammatory treatment (3). Currently, detection of coronary inflammation is hampered by a lack of specificity (e.g. serum biomarkers) or by limited availability and relatively high costs (^{18}F-FDG or ^{18}F-NaF PET) (3). Interestingly, CCTA as a widely available and utilized diagnostic tool might mediate these limitations by being able to detect changes in pericoronary adipose tissue as a response to inflammation (4). Inflamed coronaries release mediators that can lead to morphological changes of the adipocytes residing in pericoronary adipose tissue (4, 5). These alterations can be evaluated by quantifying pericoronary adipose tissue CT-attenuation (PCATa) (4). The CRISP-CT study, demonstrated that the perivascular fat attenuation index (FAI) of the right coronary artery (RCA) was of prognostic importance over clinical characteristics, qualitatively assessed extent of CAD, and HRP features (6). However, recent studies suggest superior prognostic value of quantitative plaque analysis over qualitative assessment (7, 8). Studies investigating the prognostic value of PCATa beyond quantitative plaque volume are lacking. Therefore, the present study investigated whether PCATa retained its prognostic value beyond quantitative plaque measurements and ischemia.

Methods

Study population

650 patients who underwent CCTA and [^{15}O]H_2O PET perfusion imaging at the Amsterdam UMC: Vrije Universiteit Amsterdam between 2008 and 2014 because of suspected obstructive CAD were evaluated for inclusion. Of these, 32 (5%) were excluded because of a documented history of CAD (prior myocardial infarction (MI), percutaneous coronary intervention, or coronary artery bypass grafting), whereas 25 (4%) were excluded due to uninterpretable image results. Of the remainder of patients, 54 (10%) were lost to follow-up, resulting in a study population of 539 patients (2) (Figure 1). The study complied with the Declaration of Helsinki. The local ethics committee approved the study protocol and waived the need for written informed consent.

CCTA acquisition

Images were acquired on a Gemini TF 64 PET/CT-scanner (352 patients) and on a 256-slice Brilliance iCT-scanner (187 patients) (both: Philips Healthcare, Best, The Netherlands). Prior to scanning, sublingual nitroglycerine spray was administered to all patients and metoprolol if necessary, aiming for a heart rate of <65 beats per minute. Coronary artery calcium scoring (CACS) in Agatston units was obtained during a single breath-hold on a non-contrast CT. Respective CCTA parameters for the 64-slice and 256-slice scanner entailed, a section collimation of 64*0.625mm and 128*0.625mm, a gantry rotation time of 420ms and 270ms, a tube current of 800-1000mA and 200-360mA (adjusting mA based on patient's body size), and a tube voltage of 120kVp for both. Prospective ECG-gated CCTA acquisition was applied when allowed by heartrate, triggered at 75% of the R-R interval. For visualization of the coronary lumen, a bolus of 100 mL iobitidol (Xenetix 350) was injected intravenously (5.7 mL/s) followed immediately by a 50 mL saline chaser. Scans were triggered using an automatic bolus tracking technique, with a region of interest in the descending thoracic aorta.

CCTA assessment

Coronary segments with a diameter ≥2mm were assessed by a single reader (R.S.D. or M.J.B.) blinded to clinical outcome using semi-automated software (Comprehensive Cardiac Analysis, Philips

Healthcare, Best, The Netherlands). The coronaries were evaluated using axial, multiplanar reformation, maximum intensity projection, and cross-sectional images (slice thickness 0.9mm, increment 0.50mm). The centerline and vessel contours were automatically detected and manually corrected if needed. A stenosis ≥50% was considered obstructive. The following HRP features were assessed: positive remodeling (PR), low-attenuation plaque (LAP), spotty calcification, and napkin-ring sign. The remodeling index was computed as the ratio of vessel area at the site of the maximal lesion to that of a proximal reference point, with an index >1.1 representing PR (9). LAP was defined as a plaque containing any voxel <30 Hounsfield units (HU). Spotty calcification was characterized by a calcified plaque comprising <90° of the vessel circumference and <3 mm in length (9). Napkin ring sign was defined by a plaque core with low attenuation surrounded by a rim-like area of higher attenuation (9). The presence of ≥2 HRP features defined a HRP. Quantitative plaque analyses were performed within manually designated regions. Total plaque volume (TPV) was calculated by summing volumes of separate plaques along each coronary artery. A threshold of 150 HU was used to distinguish non-calcified from calcified plaque and calculation of calcified/noncalcified plaque volume (CPV/NCPV) Supplemental Figure 1 presents a case example of quantitative plaque analysis.

PCATa

Coronaries with centerlines were segmented by a single reader blinded (M.J.B.) to clinical outcome via semi-automated software and manually corrected if needed (Comprehensive Cardiac Analysis, Philips Healthcare, Best, The Netherlands). We were, due to technical difficulties, unable to extract the segmentations of 7 RCAs, 6 left anterior descending arteries (LAD), and 7 circumflex arteries (Cx). The extracted segmentations were utilized by our PCAT research prototype (Philips Healthcare, Best, the Netherlands) to detect the coronary lumen and walls using an automated algorithm (10). The automated algorithm defined the diameter of the vessel for each point along the centerline. Using the location specific diameter, PCAT was defined as tissue with HU ranging from -190 to -30 within a single concentric layer with a radial distance from the outer vessel wall equal to the diameter of the vessel (4, 6). The first mm of tissue following the vessel wall was excluded to prevent partial volume effects and artefacts due to contrast media in the lumen. PCATa analysis of the

RCA involved the proximal 10mm to 50mm of the vessel, excluding the first 10mm to prevent noise from the aortic wall (6). Regarding the left coronary system, the proximal 40mm of the LAD and Cx were assessed, excluding the left main given its variable length and possible absence (6). Lastly, PCATa was calculated by averaging the attenuation of PCAT within region of interest of the corresponding coronary and presented as mean PCATa (HU). PCATa was obtained in <15 seconds. Figure 2 presents case examples of PCATa analyses.

$[^{15}O]H_2O$ PET

Images were acquired on a Gemini TF 64 PET/CT-scanner (Philips Healthcare, Best, The Netherlands). A dynamic perfusion scan was performed during resting as well as adenosine (140µg/kg/min) induced hyperemia using 370 MBq of $[^{15}O]H_2O$ as radioactive tracer. Low-dose CT-scans allowed for attenuation correction. Parametric images of myocardial blood flow (MBF) were generated using in-house developed software (*CardiacVUer,* Amsterdam UMC: Vrije Universiteit Amsterdam, Amsterdam, the Netherlands) (11). Vascular territories were defined according to the standardized 17-segment model of the American Heart Association. A hyperemic MBF ≤2.3 ml/min/g in two adjacent segments within a vascular territory was considered indicative of myocardial ischemia (12).

Follow-up

Follow-up data was obtained using a national registry database, medical records, and telephonic contact. The endpoint was a composite of death and non-fatal MI. Events were adjudicated in accordance with current guidelines (13). Early and late revascularization were defined as revascularization based on the initial diagnostic work-up or revascularization after an initially conservative treatment, respectively.

Statistical analysis

Statistical analyses were performed using SPSS version 26.0 (IBM SPSS Statistics, Armonk, New-York), except for the construction of time-dependent receiver operating characteristics (ROC)

curves which were performed using the survivalROC package of R (R Foundation for Statistical Computing, Vienna, Austria). Normally distributed variables are presented as mean ± standard deviation and compared between groups using independent sample t-tests. Non-normally distributed variables are presented as median with interquartile range and compared with a Mann-Whitney U test. Categorical variables are presented as frequencies with percentages and compared with the Fisher's Exact test, except for type of chest pain which was compared using the Pearson Chi-Square test. Correlations were assessed using Pearson's and Spearman's correlations when appropriate. Time-dependent ROC curves of quantitative CCTA variables for prediction of events within the first 5 years of follow-up were constructed. Optimal cut-offs were determined by maximizing the Youden-index. The first 5 years of follow-up were utilized as the majority of patients without an event (74%) had 5 year follow-up available, allowing assessment of prognostic thresholds in an adequate sample of the population. Follow-up was censored after 5 years to match the time span on which the time dependent ROC curve derived prognostic thresholds were based. Kaplan-Meier curves were plotted to visualize event-free survival and compared with Log-rank tests. Univariable Cox proportional hazard regression analyses were used to identify variables associated with outcome ($p<0.10$). Multivariable Cox proportional hazard regression analyses using backward selection and enter mode were used to assess the independent prognostic value of clinical and imaging variables. A two-sided p-value <0.05 was considered statistically significant.

Results

Patient characteristics and follow-up results

Patient characteristics and imaging results are displayed in Table 1. During a median follow-up of 5.0 [4.7-5.0] years, 17 (3%) patients suffered an MI and 16 (3%) died. Of the 17 patients that had an MI, 11 (65%) had a non-ST segment elevation myocardial infarction (NSTEMI), 5 (29%) had an ST segment elevation myocardial infarction, and 1 (6%) MI was not further specified. The RCA and LAD were the culprit in 4 (24%) patients each, whereas the Cx was the culprit in 3 (18%) patients. Four (24%) patients had an NSTEMI witout clear culprit and in 2 (11%) patients culprit vessel was not documented. In total, 109 (20%) patients underwent early revascularization and 31 (6%) underwent late revascularization.

PCATa values

RCA, LAD, and Cx PCATa values were normally distributed and differed between the 64-slice and 256-slice CT-scanner (Figure 3). RCA PCATa correlated with LAD and Cx PCATa on the 64-slice *(R*=0.480, p<0.001 and *R*=0.472, p<0.001) and 256-slice (*R*=0.354, p<0.001 and *R*=0.425, p<0.001) CT-scanner, LAD and Cx PCATa correlated on both scanners as well (*R*=0.808, p<0.001 and *R*=0.776, p<0.001) (Supplemental Figure 2).

Association of PCATa with plaque volume and perfusion

RCA, LAD, and Cx PCATa did not correlate with TPV, CPV, and NCPV of the respective coronary (Supplemental Figure 3, 4, and 5). Futhermore, hyperemic MBF of the RCA, LAD, and Cx did not correlate with PCATa of the RCA, LAD, and Cx, respectively (Supplemental Figure 6).

Association of imaging parameters with outcome

Obstructive CAD, HRPs, and ischemia were more prevalent among patient with an endpoint (Table 1). Furthermore, CACS, TPV, CPV, and NCPV were higher in patients who experienced an event as compared to those who did not, whereas PCATa did not differ between patients with and without an event. Prognostic thresholds for quantitative CCTA variables and scanner specific PCATa

thresholds are presented in Supplemental Figure 7 and 8, respectively. Obstructive CAD, HRPs, CACS >59, TPV >220mm^3, CPV >110mm^3, NCPV >85mm^3, and ischemia were associated with worse outcome (Table 2 and Figure 3). Regarding PCATa, scanner specific RCA thresholds of >-67.4 HU (64-slice CT-scanner) and >-76.3 HU (256-slice CT-scanner) were associated with outcome, whereas LAD and Cx PCATa were not associated with events (Table 2, Figure 3, and Supplemental Figure 9).

RCA PCATa as predictor of outcome

Age, diabetes mellitus, hyperlipidemia, early revascularization, and all imaging parameters were identified as variables associated with outcome (Table 2). RCT PCATa above scanner specific thresholds and NCPV >85mm^3 were of independent predictive value beyond the aforementioned variables. In a similar analyses that excluded patients that underwent early revascularization, RCA PCATa above scanner specific thresholds (HR: 2.65, 95% CI: 1.12-6.26, p=0.026), NCPV >83mm^3 (HR: 6.42, 95% CI: 2.25-18.33, p=0.001), and ischemia (HR: 2.95, 95% CI: 1.03-8.41, p=0.044) were independent predictors of events (Supplemental Table 1). RCA PCATa remained of prognostic value when separately adjusted for variables associated with outcome, clinical characteristics, and imaging parameters (Table 3). Lastly, RCA PCATa was higher among 55 patients that underwent early and/or late revascularization scanned on the 64-slice CT-scanner (-69.4±7.8 HU vs. -73.3±8.3 HU, p=0.001), but did not differ among 76 patients that underwent early and/or late revascularization scanned on the 256-slice CT-scanner (-80.3±8.1 HU vs. -80.1±7.2 HU, p=0.859).

Discussion

The present study assessed the prognostic value of PCATa beyond quantitative plaque volume and ischemia among patients with suspected CAD. RCA PCATa above scanner specific thresholds was associated with outcome. Furthermore, PET/CCTA-derived CACS, obstructive CAD, HRPs, TPV, CPV, NCPV, and myocardial ischemia were related to occurrence of death and non-fatal MI as well and were so to a greater extent as compared to RCA PCATa. Nevertheless, RCA PCATa was of prognostic value beyond clinical characteristics and imaging variables linked to extent and severity of atherosclerosis (Central illustration).

Prognostic value of plaque burden and vulnerability

In the present study markers of plaque burden and vulnerability were all associated with outcome of which NCPV was the strongest independent prognostic predictor adjusted for clinical characteristics and imaging parameters. The superior prognostic value of anatomical assessment over that of functional assessment is substantiated by substudies of the PROMISE-trial and ISCHEMIA-trial (14, 15). Regarding anatomical assessment, several studies have demonstrated that presence of obstructive CAD and HRPs are associated with detrimental outcome (2, 8, 16). However, substudies of the SCOT-HEART trial revealed that this relation might be driven by overall plaque burden as the prognostic value of obstructive disease and HRPs was dependent on CACS and as quantitative LAP burden proved to be a stronger predictor of outcome compared to obstructive CAD and CACS. (8, 17). In line with these findings, Andreini et al. show quantitative TPV, CPV, and NCPV to be of incremental prognostic value over cardiovascular risk factors and visually assessed CCTA-derived multivessel disease and similarly as the present study demonstrate NCPV to be the strongest predictor of events (7). Interestingly, RCA PCATa as a possible marker of global coronary inflammation proved to be of prognostic value over CCTA-derived parameters linked to plaque burden, vulnerability, and myocardial ischemia.

Pathophysiological mechanism of PCATa

Coronary atherosclerosis is marked by a lipid-driven inflammation, which precedes the formation of plaques (18). The inflammatory process within the coronary wall can, by excretion of pro-inflammatory cytokines, impede the maturation and thereby influence the size of the adipocytes in the surrounding PCAT (4). The balance between the lipid and aqueous phases of PCAT is largely dependent on adipocyte size, wherein larger adipocytes have an increased lipid content (4, 19). CT-derived attenuation values of adipose tissue can therefore be used to assess the phenotype of PCAT (4). PCATa is inversely associated with adipose differentiation and size, i.e. the lower the attenuation (HU closer to -190) the larger the adipocytes (4). Pro-inflammatory signals excreted by inflamed coronaries inhibit maturation of adipocytes and lead to smaller more aqueous adipocytes and a higher PCATa (HU closer to -30) (4).

Association of PCATa with CAD and perfusion

Antonopoulos et al. demonstrate RCA PCATa to correlate with atherosclerotic plaque burden but not with calcification volume of the underlying coronary segment (4). Furthermore, RCA PCATa predicted presence of obstructive CAD in any of the coronaries, independent of CACS (4). High PCATa has also been associated with impaired coronary flow reserve on PET perfusion imaging, a relationship that was independent of cardiovascular risk factors, CACS, and presence of obstructive CAD (20). Interestingly, this association persevered among patients with low CACS or non-obstructive CAD, indicating that PCATa may identify ‘low-risk’ patients prone to ischemia (20). In contrast, the present study does not observe an association between PCATa and plaque volume nor hyperemic MBF. Our study included patients with CAD ranging from non-existent to extensive multivessel CAD. Although speculative, patients with no or a low plaque burden might have high PCATa as expression of beginning atherosclerosis, whereas patients with extensive CAD can have high PCATa delineating ongoing inflammation or low PCATa as a result of an extinguished inflammatory response due to e.g. medical therapy. Notably, in the present study 66% and 75% of patients were prescribed statins and acetylsalicylic acid at baseline, respectively. This might explain the absence of association between PCATa, plaque volume, and perfusion. As PCATa highlights ongoing inflammation it might be more suitable to describe progression of CAD (21). In line with this

statement, Goeller et al. show baseline RCA PCATa to be independently associated with an increase in NCP burden and demonstrate changes in RCA PCATa to correlate with changes in NCP burden and low-density NCP burden assessed on serial CCTA (21). Noteworthy, a decrease in PCATa among patients in which statin therapy was initiated was observed (21).

Prognostic value of PCATa

In the CRISP-CT study PCATa was incorporated in calculating the FAI using a proprietary algorithm (*CaRiHEART*, Caristo Diagnostics, Oxford, United Kingdom) (3, 6). FAI of the RCA and LAD were associated with all-cause and cardiac mortality, whereas FAI Cx was associated with all-cause but not cardiac mortality (6). High FAI RCA (≥-70.1 HU), as a suggested marker of global coronary inflammation, was predictive of all-cause and cardiac mortality beyond clinical characteristics, epicardial adipose tissue volume, number of HRP features, and Duke index for extent of CAD (6). The increased risk of all-cause mortality in patients with high FAI was driven by a higher rate of cardiac deaths and not in non-cardiac deaths (6). We corroborate these findings by demonstrating that RCA PCATa above scanner specific thresholds was independently associated with occurrence of death and non-fatal MI. The scanner specific RCA PCATa thresholds of the present study identify relatively outlying PCATa values. These 'abnormal' values are associated with events to a greater extent as compared to PCATa values below the cut-off. However, it should be noted that given the similar RCA PCATa of patients with and without an event and the discriminating ability of the ROC curves, RCA PCATa as a sole prognostic determinant might not be useful for risk stratification but should possibly be utilized in conjunction with other CAD markers. This is illustrated by a substudy of the CRISP-CT study in which patients with high FAI and HRP features were at an increased risk of suffering events, whereas patients with low FAI and HRP features were not (22). The association of RCA PCATa with all-cause mortality is possibly, similar to the CRISP-CT study, driven by a higher rate of cardiac deaths (6). The association of PCATa with MI has previously been substantiated by Goeller et al. who observed higher PCATa values surrounding culprit lesions of MI patients as compared to non-culprit lesions, healthy controls, and patients with stable CAD (4, 23). We extent the findings of the CRISP-CT study by demonstrating that RCA PCATa retains its prognostic

value beyond quantitative plaque volume, high-risk plaques, and myocardial ischemia. Contrary to the CRISP-CT study, LAD and Cx PCATa were not associated with event-free survival. This is in line with the study of Bengs et al. in which RCA PCATa was associated with occurrence of events, whereas LAD and left main PCATa were not (24). A possible explanation for this discordancy is the fact that PCAT is more prevalent around the RCA as compared to the left coronary system and has less hindering non-fatty structures (e.g. side branches and myocardium) in its proximity (4, 21, 25). Therefore RCA PCATa might be a more robust and easily accessible measurement of global inflammatory status and it might explain the superior prognostic value as compared to PCATa of the LAD and Cx.

Future prospects

Recent randomized trials highlight inflammation as an important risk-factor in patients with CAD by demonstrating that anti-inflammatory treatment reduces events rates as compared to placebo (26-28). Identifying patients at a "high" inflammatory risk might further improve outcome (3). Interestingly, in the CRISP-CT study, the increased risk of cardiac mortality in patients with high FAI was nullified among those that received the recommendation to initiate treatment with statins and aspirin, whereas the risk was 18-fold higher in patients with high FAI that did not change medical regime (6). Furthermore, inflammation is a dynamic process and PCATa/FAI might be utilized to monitor the effect of treatment. PCATa around culprit lesions of MI patients is elevated and diminishes overtime, possibly indicating an effect of commenced medical treatment (4). Furthermore, Elnabawi et al. demonstrate that in patients with psoriasis, FAI diminishes among those on anti-inflammatory medication while no change is observed in those that are not (29).

Limitations

The power of the study is hampered by the low number of events. In this regard, the multivariable analyses should be interpreted with causing as they are prone to overfitting given the relatively large number of predictors that were included. Results should be seen as hypothesis generating and need further validation. To that extent, the provided prognostic cut-offs for CCTA

variables should not be extrapolated to other datasets but serve to show the incremental prognostic value of PCATa on top of other CCTA variables for which optimal cut-offs were calculated as well. Prognostic thresholds for PCATa should be assessed in larger CCTA cohorts and validated in independent cohorts taking into account scanner differences. Obstructive CAD is defined as ≥50% stenosis, which can be considered low on CCTA. Next, PCATa is defined as the average attenuation of PCAT, which might result in an underestimation of coronary inflammation in obese individuals as attenuation will be lower given the larger adipocytes, vice versa this can lead to an overestimation in lean patients (3). Furthermore, PCATa is assumed to be a marker of coronary inflammation however the present study lacks data to confirm the presence of coronary inflammation by means of e.g. PET imaging. Next, despite the fact that an early invasive strategy does not seem to alter outcome regardless of the anatomical severity of CAD or degree of ischemia, inclusion of patients that underwent early revascularization might have introduced unmeasured confounding (15). Lastly, the present study uses a composite endpoint of death and non-fatal MI but does not provide information on cause of death as this was unavailable.

Conclusion

Parameters associated with atherosclerotic burden and ischemia were more strongly associated with outcome than RCA PCATa. Nonetheless, RCA PCATa above scanner specific thresholds, as a marker of global coronary inflammation, provides incremental prognostic value beyond clinical characteristics, CACS, obstructive CAD, HRPs, quantitative plaque volume, and myocardial ischemia.

Perspectives

Competency in Medical Knowledge

Coronary inflammation plays a pivotal role in atherosclerosis. PCATa is a novel marker of coronary inflammation and might be an interesting future treatment target. RCA PCATa, as a marker of global coronary inflammation, is of prognostic value independent of clinical characteristics, CACS, obstructive CAD, HRPs, TPV, CPV, NCPV, and ischemia.

Translational outlook

Future studies are warranted to validate PCATa as a prognostic marker and to assess whether PCATa targeted medical treatment will result in improved outcome in patients with CAD.

References

1. Knuuti J, Wijns W, Saraste A, et al. 2019 ESC Guidelines for the diagnosis and management of chronic coronary syndromes. Eur Heart J. 2020;41(3):407-77.

2. Driessen RS, Bom MJ, van Diemen PA, et al. Incremental prognostic value of hybrid [15O]H2O positron emission tomography-computed tomography: combining myocardial blood flow, coronary stenosis severity, and high-risk plaque morphology. Eur Heart J Cardiovasc Imaging. 2020;21(10):1105-13.

3. Antoniades C, Antonopoulos AS, Deanfield J. Imaging residual inflammatory cardiovascular risk. Eur Heart J. 2020;41(6):748-758.

4. Antonopoulos AS, Sanna F, Sabharwal N, et al. Detecting human coronary inflammation by imaging perivascular fat. Sci Transl Med. 2017;9(398).

5. Mazurek T, Zhang LF, Zalewski A, et al. Human epicardial adipose tissue is a source of inflammatory mediators. Circulation. 2003;108(20):2460-6.

6. Oikonomou EK, Marwan M, Desai MY, et al. Non-invasive detection of coronary inflammation using computed tomography and prediction of residual cardiovascular risk (the CRISP CT study): a post-hoc analysis of prospective outcome data. The Lancet. 2018;392(10151):929-39.

7. Andreini D, Magnoni M, Conte E, et al. Coronary Plaque Features on CTA Can Identify Patients at Increased Risk of Cardiovascular Events. JACC Cardiovasc Imaging. 2020;13(8):1704-17.

8. Williams MC, Kwiecinski J, Doris M, et al. Low-Attenuation Noncalcified Plaque on Coronary Computed Tomography Angiography Predicts Myocardial Infarction: Results From the Multicenter SCOT-HEART Trial (Scottish Computed Tomography of the HEART). Circulation. 2020;141(18):1452-62.

9. Bom MJ, van der Heijden DJ, Kedhi E, et al. Early Detection and Treatment of the Vulnerable Coronary Plaque: Can We Prevent Acute Coronary Syndromes? Circ Cardiovasc Imaging. 2017;10(5): e005973.

10. Freiman M, Nickisch H, Prevrhal S, et al. Improving CCTA-based lesions' hemodynamic significance assessment by accounting for partial volume modeling in automatic coronary lumen segmentation. Med Phys. 2017;44(3):1040-9.

11. Harms HJ, Knaapen P, de Haan S, et al. Automatic generation of absolute myocardial blood flow images using [15O]H2O and a clinical PET/CT scanner. Eur J Nucl Med Mol Imaging. 2011;38(5):930-9.

12. Danad I, Raijmakers PG, Driessen RS, et al. Comparison of Coronary CT Angiography, SPECT, PET, and Hybrid Imaging for Diagnosis of Ischemic Heart Disease Determined by Fractional Flow Reserve. Jama Cardiology. 2017;2(10):1100-7.

13. Knuuti J, Wijns W, Saraste A, et al. 2019 ESC Guidelines for the diagnosis and management of chronic coronary syndromes. European Heart Journal. 2019;00:1-71.

14. Hoffmann U, Ferencik M, Udelson JE, et al. Prognostic Value of Noninvasive Cardiovascular Testing in Patients With Stable Chest Pain: Insights From the PROMISE Trial (Prospective Multicenter Imaging Study for Evaluation of Chest Pain). Circulation. 2017;135(24):2320-32.

15. Maron D. Relationships of ischemia severity and coronary artery disease extent with clinical outcomes in the ISCHEMIA trial. Paper presented at: The American College of Cardiology Sientific Sessions. March 2020.

16. Chang HJ, Lin FY, Lee SE, et al. Coronary Atherosclerotic Precursors of Acute Coronary Syndromes. J Am Coll Cardiol. 2018;71(22):2511-22.

17. Williams MC, Moss AJ, Dweck M, et al. Coronary Artery Plaque Characteristics Associated With Adverse Outcomes in the SCOT-HEART Study. J Am Coll Cardiol. 2019;73(3):291-301.

18. Ross R. Atherosclerosis--an inflammatory disease. N Engl J Med. 1999;340(2):115-26.

19. DiGirolamo M, Owens JL. Water content of rat adipose tissue and isolated adipocytes in relation to cell size. Am J Physiol. 1976;231(5 Pt. 1):1568-72.

20. Nomura CH, Assuncao-Jr AN, Guimarães PO, et al. Association between perivascular inflammation and downstream myocardial perfusion in patients with suspected coronary artery disease. Eur Heart J Cardiovasc Imaging. 2020;21(6):599-605.

21. Goeller M, Tamarappoo BK, Kwan AC, et al. Relationship between changes in pericoronary adipose tissue attenuation and coronary plaque burden quantified from coronary computed tomography angiography. Eur Heart J Cardiovasc Imaging. 2019;20(6):636-43.

22. Oikonomou EK, Desai MY, Marwan M, et al. Perivascular Fat Attenuation Index Stratifies Cardiac Risk Associated With High-Risk Plaques in the CRISP-CT Study. J Am Coll Cardiol. 2020;76(6):755-7.

23. Goeller M, Achenbach S, Cadet S, et al. Pericoronary Adipose Tissue Computed Tomography Attenuation and High-Risk Plaque Characteristics in Acute Coronary Syndrome Compared With Stable Coronary Artery Disease. JAMA Cardiol. 2018;3(9):858-63.

24. Bengs S, Haider A, Warnock GI, et al. Quantification of perivascular inflammation does not provide incremental prognostic value over myocardial perfusion imaging and calcium scoring. Eur J Nucl Med Mol Imaging. 2020.

25. Balcer B, Dykun I, Schlosser T, et al. Pericoronary fat volume but not attenuation differentiates culprit lesions in patients with myocardial infarction. Atherosclerosis. 2018;276:182-8.

26. Ridker PM, Everett BM, Thuren T, et al. Antiinflammatory Therapy with Canakinumab for Atherosclerotic Disease. N Engl J Med. 2017;377(12):1119-31.

27. Tardif JC, Kouz S, Waters DD, et al. Efficacy and Safety of Low-Dose Colchicine after Myocardial Infarction. N Engl J Med. 2019;381(26):2497-505.

28. Nidorf SM, Fiolet ATL, Mosterd A, et al. Colchicine in Patients with Chronic Coronary Disease. N Engl J Med. 2020; doi: 10.1007/s00259-020-05106-0.

29. Elnabawi YA, Oikonomou EK, Dey AK, et al. Association of Biologic Therapy With Coronary Inflammation in Patients With Psoriasis as Assessed by Perivascular Fat Attenuation Index. JAMA Cardiol. 2019;4(9):885-891.

Figure legends

Central illustration. The present study assessed the prognostic value of PCATa among 539 patients with suspected CAD that underwent CCTA and [^{15}O]H_2O PET perfusion imaging. Imaging assessment consisted of CACS, presence of obstructive CAD and HRPs, TPV, CPV, NCPV, PCATa, and myocardial ischemia. Prognostic thresholds were determined for quantitative CCTA variables. All imaging variables were associated with events. With regard to PCATa, only RCA PCATa above scanner specific thresholds was associated with detrimental outcome in terms of death and non-fatal MI and remained a significant predictor of events adjusted for clinical characteristics and imaging parameters. Abbreviations; CACS: coronary artery calcium score, CAD: coronary artery disease, CCTA: coronary computed tomography angiography, CPV: calcified plaque volume, HR: hazard-ratio, HRP: high-risk plaque, HU: Hounsfield units, MI: myocardial infarction, NCPV: non-calcified plaque volume, PCATa: pericoronary adipose tissue CT-attenuation, PET: positron emission tomography, RCA: right coronary artery, TPV: total plaque volume.

Figure 1. Flowchart of the included study population. Abbreviations; CABG: coronary artery bypass grafting, PCI: percutaneous coronary intervention, other abbreviations as in Central illustration.

Figure 2. Case examples of RCA, LAD, and Cx PCATa analyses. Coronary lumen and wall were automatically detected based on semi-automated coronary segmentation and centerlines. An automated algorithm defined the diameter of the vessel for each point along the centerline. PCAT was defined as tissue with HU ranging from -190 to -30 within a single concentric layer with a radial distance from the outer vessel wall equal to the diameter of the vessel of which the first mm following the coronary wall was excluded. PCATa analysis of the right coronary artery (RCA) involved the proximal 10mm to 50mm of the vessel, excluding the first 10mm to prevent noise from the aortic wall. Regarding the left coronary system, the proximal 40mm of the left anterior descending artery (LAD) and circumflex artery (Cx) were assessed, excluding the left main given its variable length and possible absence. PCATa was calculated by averaging the attenuation of PCAT within the region of interest of the

corresponding coronary and presented as mean PCATa (HU). Abbreviations; Cx: circumflex artery, LAD: left anterior descending artery, other abbreviations as in Central Illustration.

Figure 3. Histograms of absolute frequencies of PCATa values stratified for CT-scanner. Figure 3 demonstrated the distribution of RCA, LAD, and Cx PCATa values stratified for scanner type. Mean PCATa values differed significantly between scanners. Abbreviations as in Central illustration.

Figure 4. Prognostic value of imaging variables. Figure 4 demonstrates the association of imaging variables with event-free survival presented by Kaplan-Meier curves with corresponding Log-rank p-values. Abbreviations as in Central Illustration.

Table 1. Patient and imaging characteristics.

	Overall (N=539)	No event (N=506)	Event (N=33)	p-value
Demographics				
Age, years	58.6 ± 9.2	58.3 ± 9.2	62.5 ± 7.4	0.011
Male	297 (55%)	275 (54%)	22 (67%)	0.207
BMI, kg/m^2	27.0 ± 4.1	27.0 ± 4.2	26.3 ± 3.1	0.287
Cardiovascluar risk factors				
Diabetes Mellitus	94 (17%)	84 (17%)	10 (30%)	0.059
Hypertension	251 (47%)	232 (46%)	19 (58%)	0.280
Hyperlipidemia	196 (36%)	179 (35%)	17 (52%)	0.092
Current smoker	184 (34%)	173 (34%)	11 (33%)	>0.999
Family history of CAD	286 (53%)	270 (53%)	16 (49%)	0.591
Type of chestpain				0.325
Typical angina	165 (31%)	154 (30%)	11 (33%)	-
Atypical angina	188 (35%)	174 (34%)	14 (42%)	-
Non-specific chestpain	180 (33%)	173 (34%)	7 (21%)	-
Medication				
Statin	356 (66%)	329 (65%)	27 (82%)	0.059
Acetylsalicylic acid	404 (75%)	374 (74%)	30 (91%)	0.036
Beta-blocker	325 (60%)	299 (59%)	26 (79%)	0.041
ACE-inhibitor/ARB	190 (35%)	173 (34%)	17 (52%)	0.060
Calcium-channel blocker	141 (26%)	126 (25%)	15 (46%)	0.014
PET perfusion imaging	N=539	N=506	N=33	
Indicative of ischemia	259 (48%)	233 (46%)	26 (79%)	<0.001
CCTA	N=535	N=503	N=32	
CACS, Agatston	53 [0-312]	44 [0-287]	330 [89-1418]	<0.001
Qualitative results	N=539	N=506	N=33	

Obstructive CAD	302 (56%)	274 (54%)	28 (85%)	<0.001
High-risk plaque	127 (24%)	111 (22%)	16 (49%)	0.001
Quantitative results	N=539	N=506	N=33	
TPV, mm^3	166 [14-489]	148 [9-430]	506 [302-878]	<0.001
CPV, mm^3	95 [6-316]	79 [3-299]	300 [152-628]	<0.001
NCPV, mm^3	48 [2-148]	40 [1-135]	201 [106-284]	<0.001
64-slice CT-scanner				
RCA PCATa, HU	-72.7 ± 8.4 (N=347)	-72.9 ± 8.4 (N=322)	-70.0 ± 8.1 (N=25)	0.097
RCA PCATa >-67.4 HU	100 (28%)	88 (27%)	12 (48%)	0.038
LAD PCATa, HU	-76.4 ± 8.0 (N=351)	-76.5 ± 8.0 (N=326)	-74.7 ± 7.9 (N=25)	0.286
Cx PCATa, HU	-74.6 ± 8.2 (N=348)	-74.7 ± 8.3 (N=323)	-74.2 ± 7.0 (N=25)	0.778
256-slice CT scanner				
RCA PCATa, HU	-80.2 ± 7.7 (N=185)	-80.3 ± 7.6 (N=177)	-78.7 ± 11.2 (N=8)	0.697
RCA PCATa >-76.3 HU	49 (26%)	44 (25%)	5 (63%)	0.032
LAD PCATa, HU	-84.5 ± 7.2 (N=182)	-84.4 ± 7.2 (N=174)	-87.2 ± 5.9 (N=8)	0.274
Cx PCATa, HU	-83.9 ± 7.3 (N=184)	-83.8 ± 7.2 (N=176)	-87.1 ± 8.6 (N=8)	0.216

Values are expressed as mean ± SD, median [IQR], or numbers (%).

Abbreviations; ACE: angiotensine converting enzyme, ARB: angiotensine receptor blocker, BMI: body mass index, CACS: coronary artery calcium score, CAD: coronary artery disease, CPV: calcified plaque volume, Cx: cicumflex artery, HU: Houndsfield units, IQR: interquartile range, LAD: left anterior descending artery, MI: myocardial infarction, MBF: myocardial blood flow, NCPV: non-calcified plaque volume, PCATa: pericoronary addipose tissue CT-attenuation, RCA: right coronary artery, SD: standard deviation, TPV: total plaque volume.

Table 2. Univariable and multivariable cox proportional hazard regression analyses for determing predictors of events.

	Univariable analyses		Multivariable analysis (backward selection)	
	HR (95% CI)	**p-value**	**HR (95% CI)**	**p-value**
Patient characteristics				
Age, years	1.05 (1.01-1.09)	0.012	-	-
Male gender	1.73 (0.84-3.56)	0.139		
Body mass index, kg/m^2	0.95 (0.87-1.04)	0.291		
Smoking	0.89 (0.43-1.83)	0.748		
Hypertension	1.54 (0.77-3.06)	0.223		
Diabetes Mellitus	2.06 (0.98-4.32)	0.057	-	-
Hyperlipidemia	1.85 (0.93-3.66)	0.078	-	-
Family history of CAD	0.81 (0.41-1.60)	0.544		
Treatment				
Early revascularization	2.22 (1.07-4.58)	0.031	-	-
PET perfusion imaging				
Indicative of ischemia	4.25 (1.84-9.78)	0.001	-	-
CCTA results				
CACS >59 Agatston	4.17 (1.80-9.64)	0.001	-	-
Qualitative results				
Obstructive CAD	4.88 (1.88-12.65)	0.001	-	-
High-risk plaque	3.41 (1.72-6.75)	<0.001	-	-
Quantitative results				
TPV >220 mm^3	7.91 (3.05-20.49)	<0.001	-	-
CPV >110 mm^3	5.82 (2.40-14.10)	<0.001	-	-
NCPV >85 mm^3	8.07 (3.33-19.55)	<0.001	9.13 (3.51-23.73)	<0.001
PCATa				

RCA PCATa above scanner specific threshold	2.84 (1.44-5.63)	0.003	2.45 (1.23-4.93)	0.011

Abbreviations; HR: hazard ratio, CI: confidence interval, other abbriations as in table 1.

Table 3. Risk of suffering an endpoint for RCA PCATa above scanner specific thresholds adjusted for clinical chacteristics and imaging variables.

	Risk of death and non-fatal myocardial infarction					
	HR[a] (95% CI)	**p-value**	**HR[b] (95% CI)**	**p-value**	**HR[c] (95% CI)**	**p-value**
RCA PCATa above scanner specific thresholds	2.37 (1.17-4.78)	0.017	2.43 (1.21-4.88)	0.012	2.38 (1.19-4.79)	0.015

[a]Adjusted in a multivariable Cox proportional hazard regression analysis using the enter method for clinical and imaging variables associated with outcome in univariable Cox proportional hazard regression analyses: age, diabetes mellitus, hyperlipidemia, early revascularization, PET indicative of ischemia, CACS >59, obstructive CAD, high-risk plaques, TPV >220 mm^3, CPV >110 mm^3, and NCPV >85 mm^3.

[b]Adjusted in a multivariable Cox proportional hazard regression analysis using the enter method for all clinical characteristics: age, gender, BMI, smoking, hypertension, diabetes mellitus, hyperlipidemia, family history of CAD, and early revascularization.

[c] Adjusted in a multivariable Cox proportional hazard regression analysis using the enter method for all imaging parameters: PET indicative of ischemia, CACS >59, obstructive CAD, high-risk plaques, TPV >220 mm^3, CPV >110 mm^3, and NCPV >85 mm^3.

Abbreviations as in table 1 and 2.

Prognostic value of RCA pericoronary adipose tissue CT-attenuation beyond high-risk plaques, plaque volume, and myocardial ischemia

Study population: 539 patients who underwent CCTA and [^{15}O]H_2O PET perfusion imaging because of suspected CAD

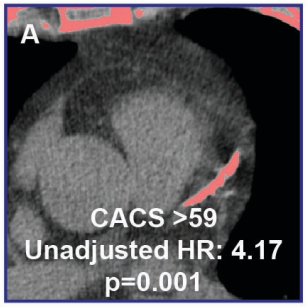

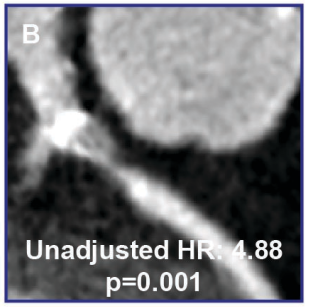

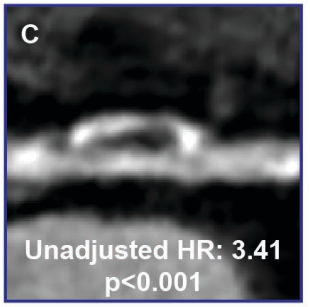

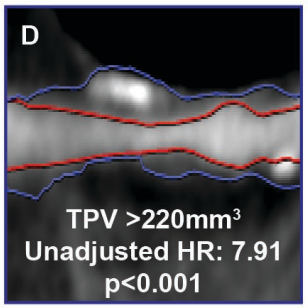

CCTA/PET assessment:
Coronary artery calcium score (A)
Obstructive disease (B)
High-risk plaques (C)
Total plaque volume (D)
Calcified plaque volume (E)
Noncalcified plaque volume (F)
PET indicative of ischemia (G)
Pericoronary adipose tissue CT-attenuation (H)

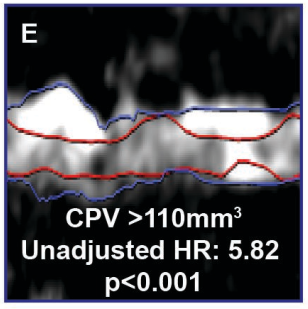

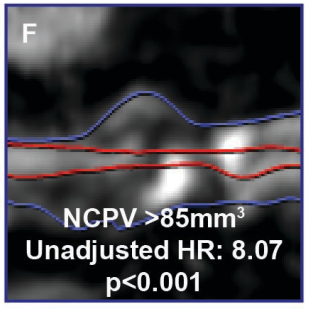

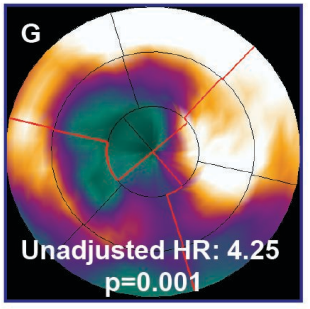

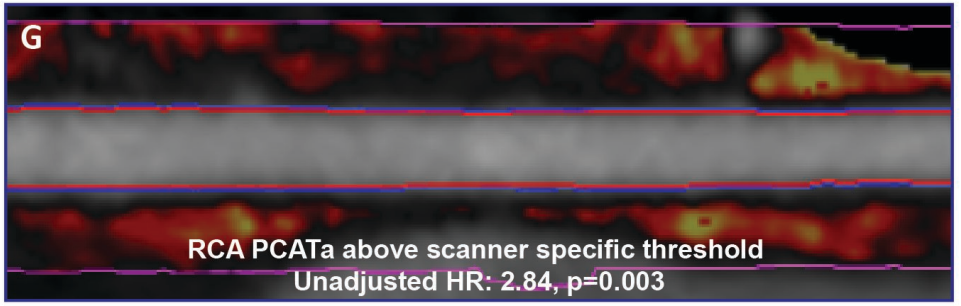

Follow-up
During a median follow up of 5.0 [4.7-5.0] years
33 patients suffered an event (death/non-fatal MI)

Prognostic value of RCA PCATa

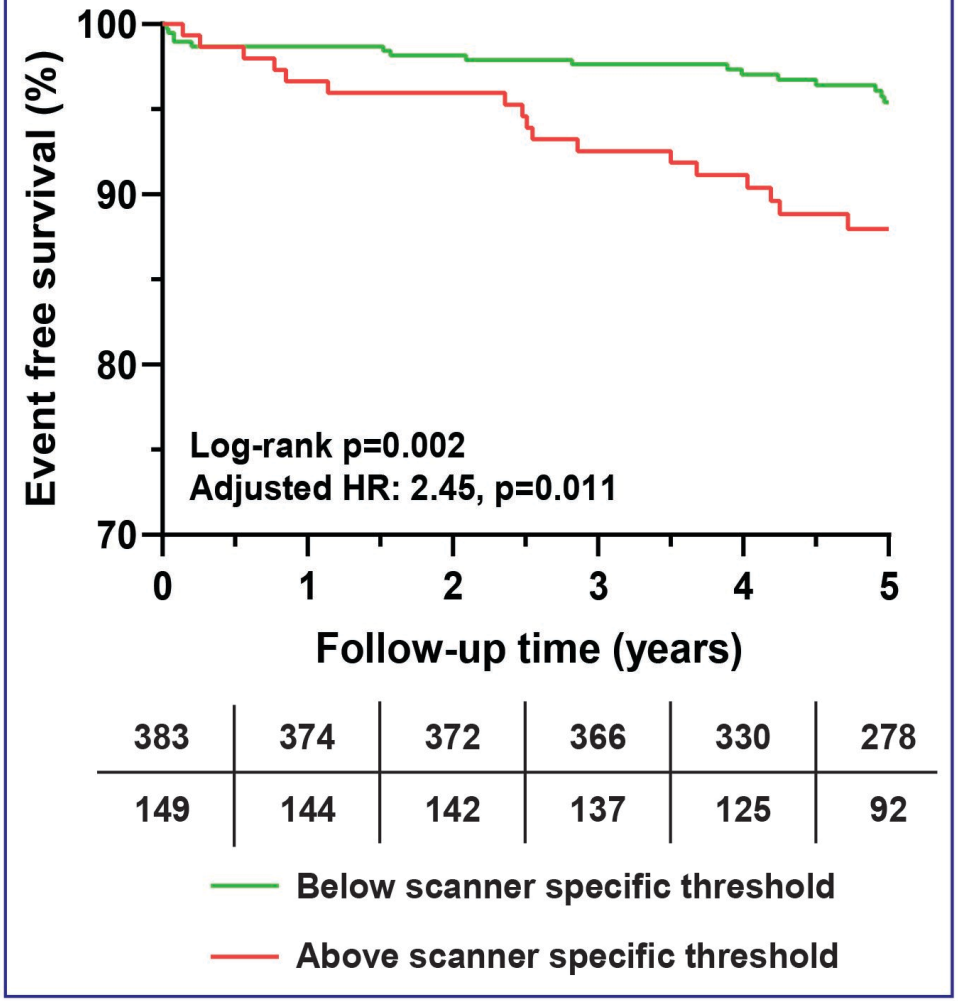

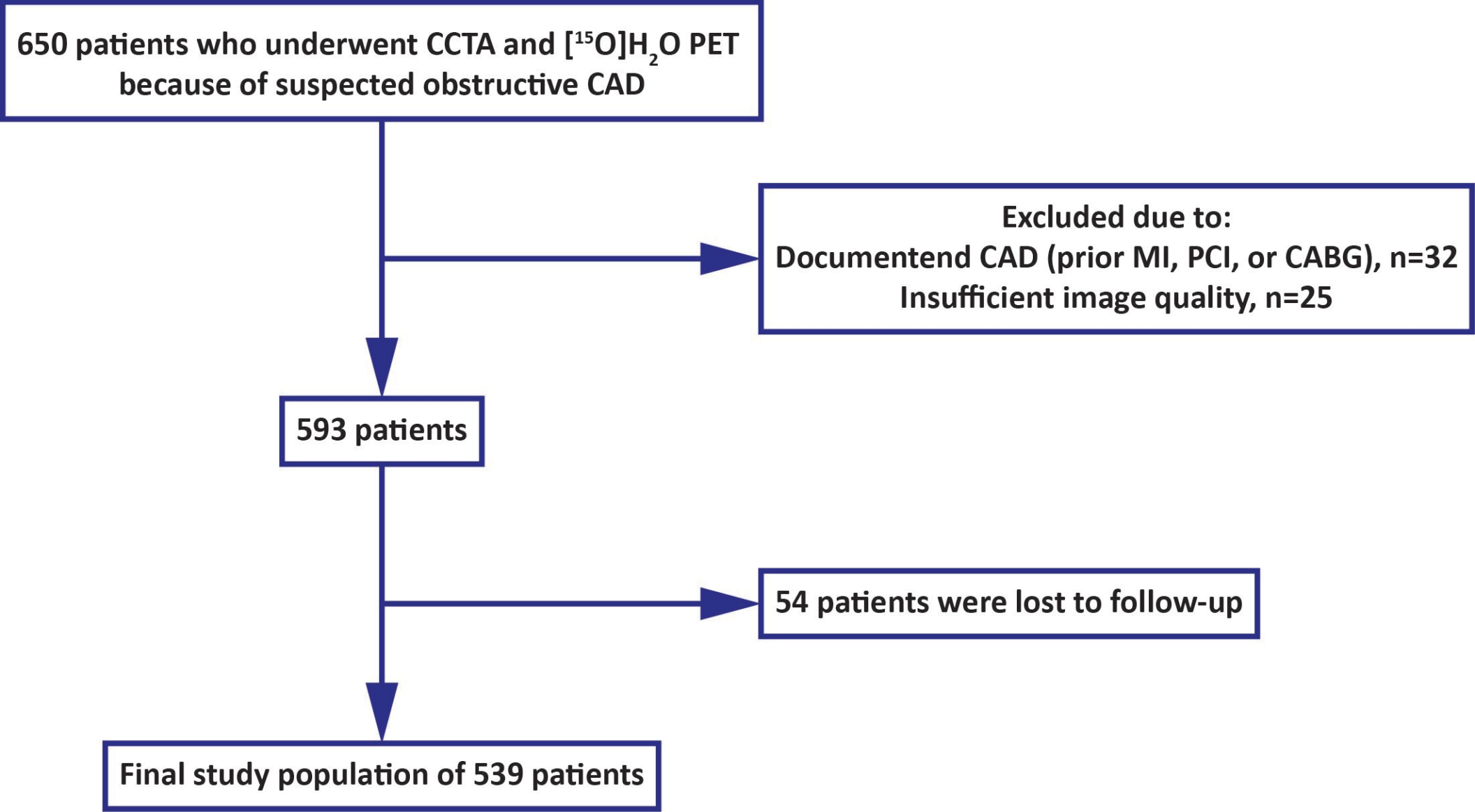
650 patients who underwent CCTA and [15O]H2O PET because of suspected obstructive CAD
Excluded due to:
Documentend CAD (prior MI, PCI, or CABG), n=32
Insufficient image quality, n=25
593 patients
54 patients were lost to follow-up
Final study population of 539 patients

PCATa analysis of the RCA

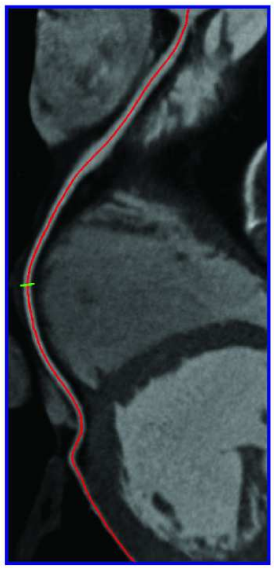

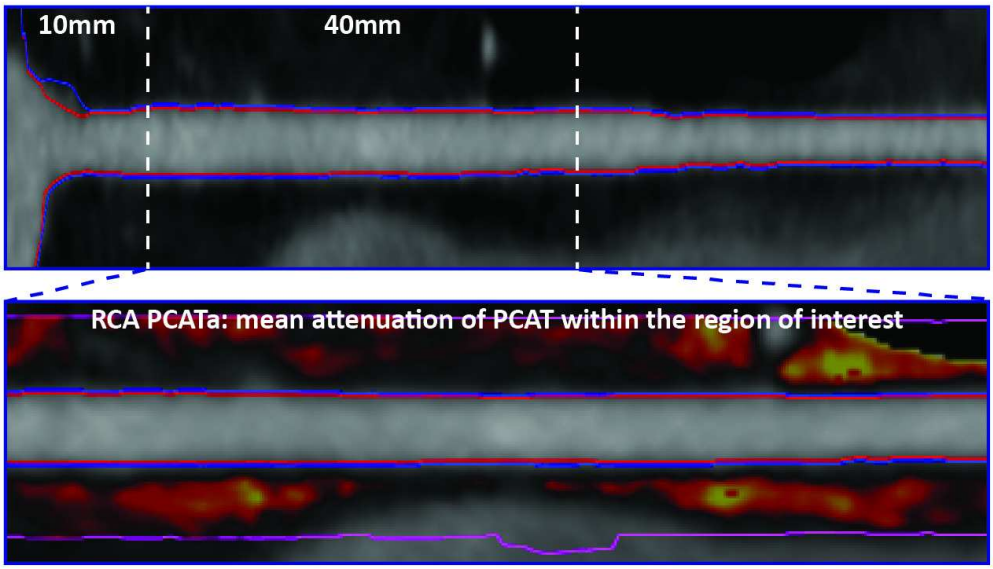

PCATa analysis of the LAD

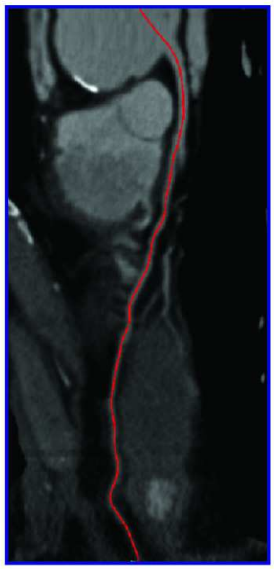

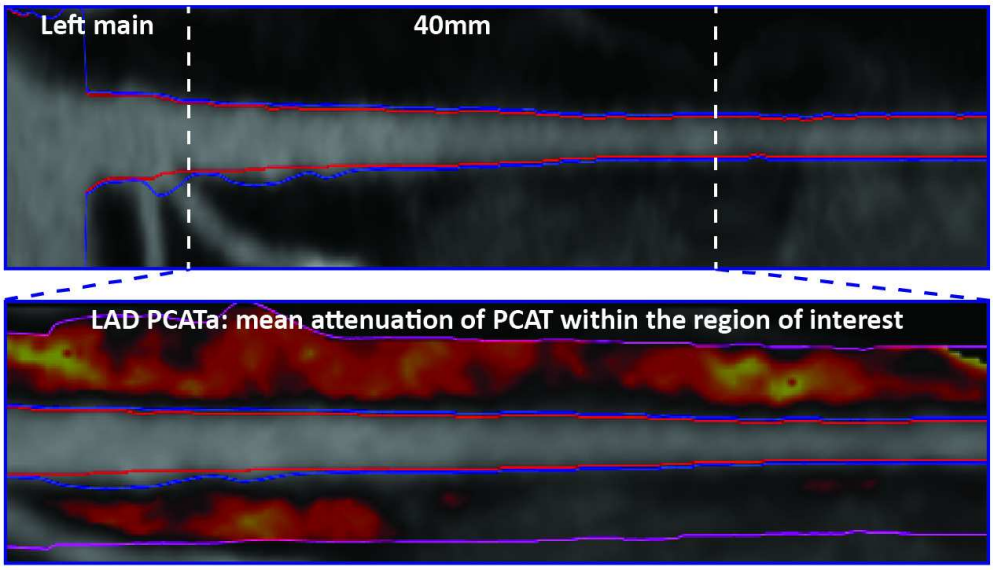

PCATa analysis of the Cx

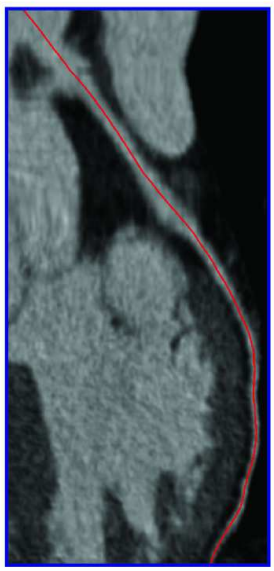

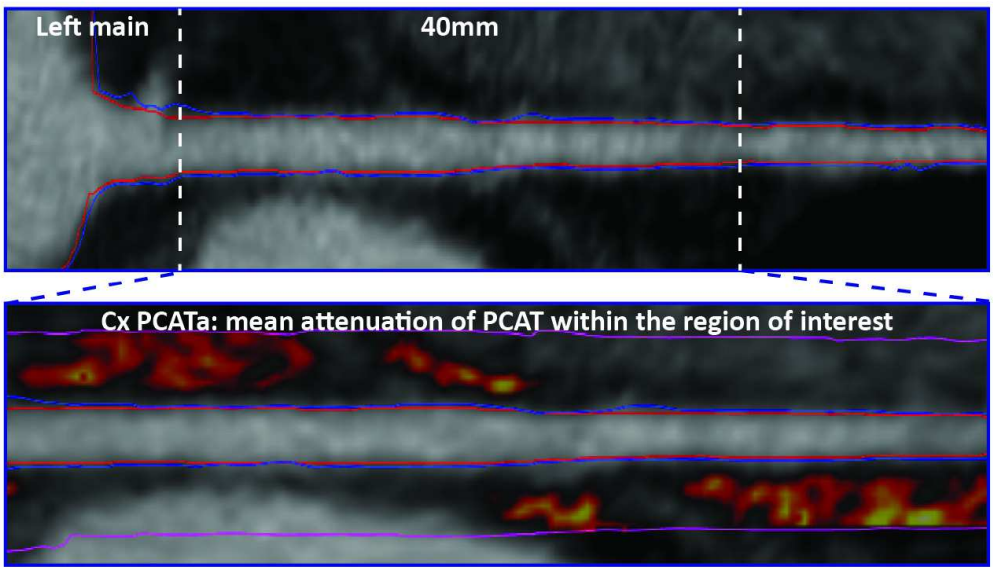

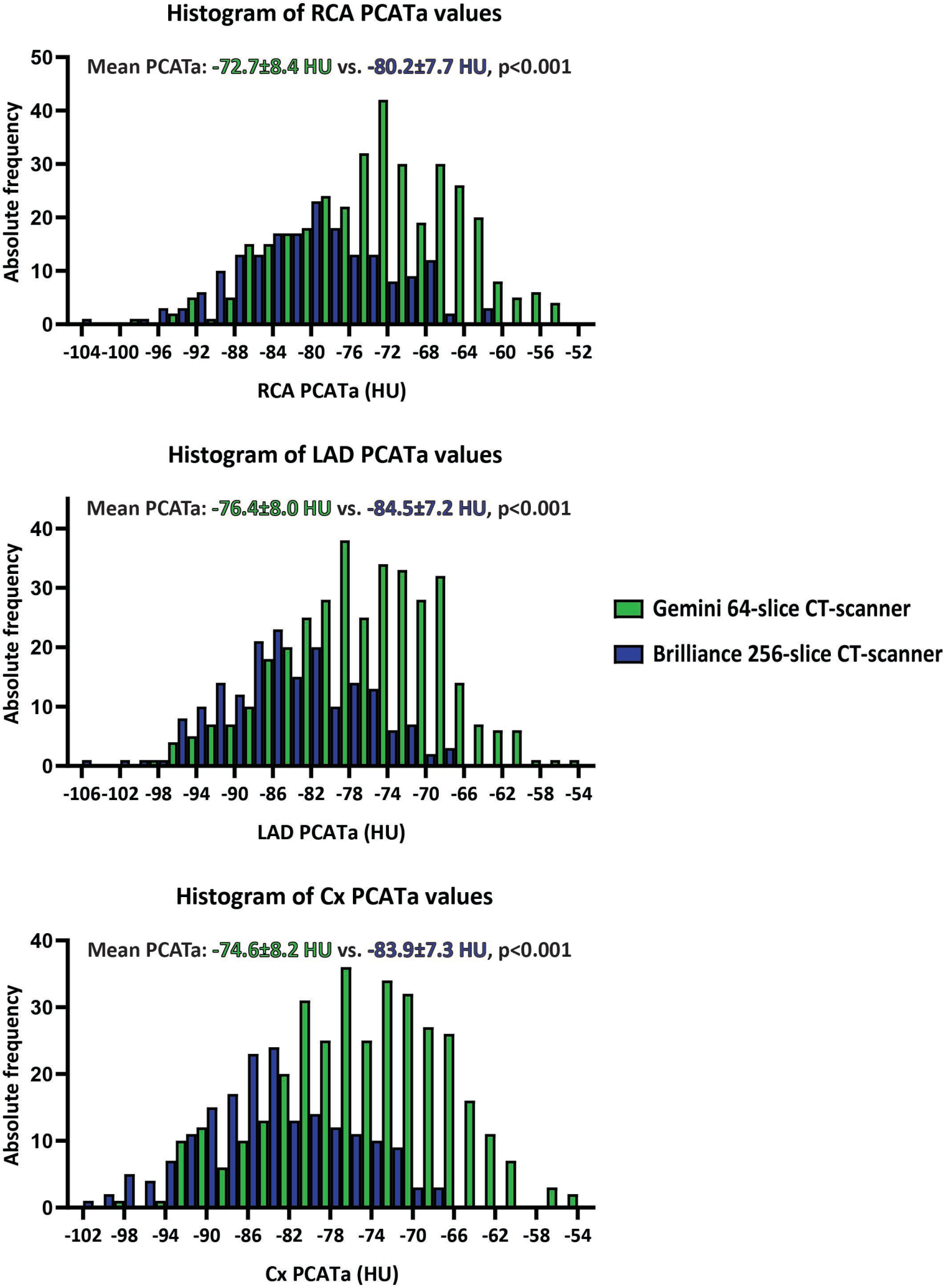
Histogram of RCA PCATa values
Mean PCATa: -72.7±8.4 HU vs. -80.2±7.7 HU, p<0.001
Absolute frequency
RCA PCATa (HU)
Histogram of LAD PCATa values
Mean PCATa: -76.4±8.0 HU vs. -84.5±7.2 HU, p<0.001
Absolute frequency
LAD PCATa (HU)
Histogram of Cx PCATa values
Mean PCATa: -74.6±8.2 HU vs. -83.9±7.3 HU, p<0.001
Absolute frequency
Cx PCATa (HU)
Gemini 64-slice CT-scanner
Brilliance 256-slice CT-scanner

Coronary artery calcium score

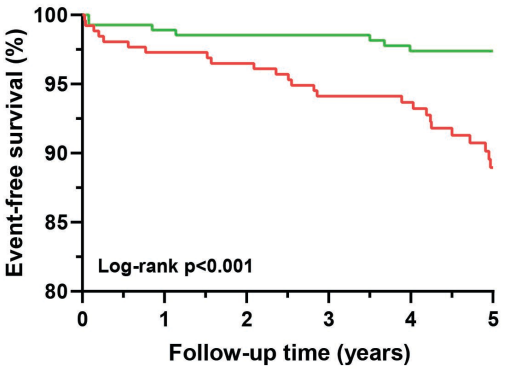

≤59 Agatston	275	272	270	267	248	226
>59 Agatston	260	249	249	239	210	146

Obstructive CAD

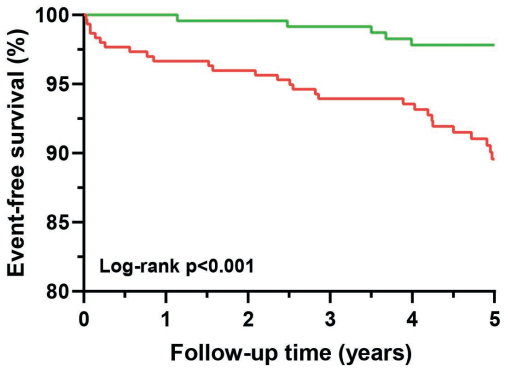

237	237	236	233	218	196	No/non-obstructive CAD
302	287	284	276	243	179	Obstructive CAD

High-risk plaque

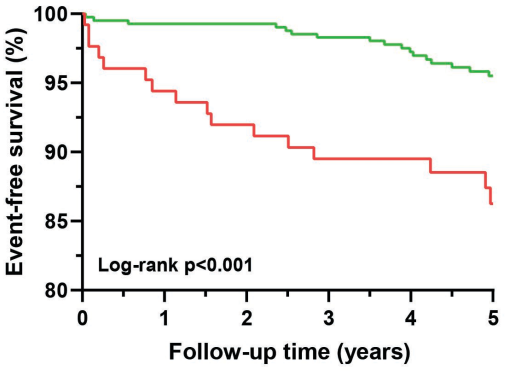

No high-risk plaque	412	408	406	399	365	300
High-risk plaque	127	117	114	110	96	75

Total plaque volume

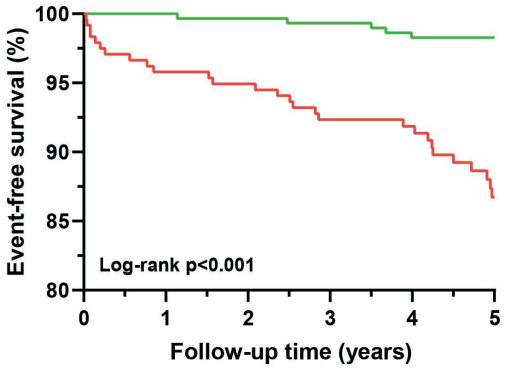

299	299	298	294	274	242	≤220 mm³
240	225	222	215	187	133	>220 mm³

Calcified plaque volume

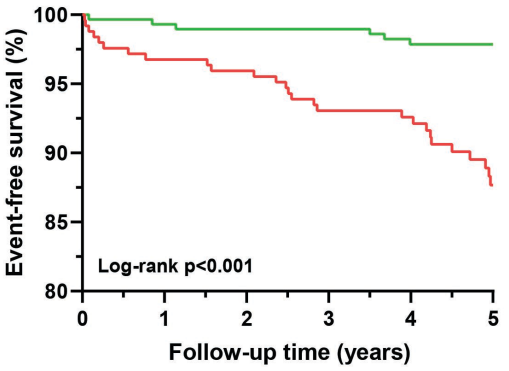

≤110 mm³	290	287	285	282	263	236
>110 mm³	249	238	235	227	198	139

Non-calcified plaque volume

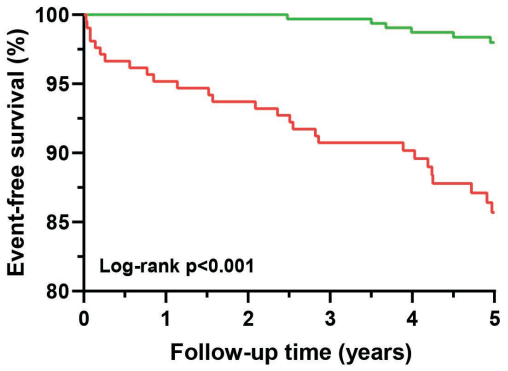

329	329	328	325	303	257	≤85 mm³
210	195	192	184	158	118	>85 mm³

PET indicative of ischemia

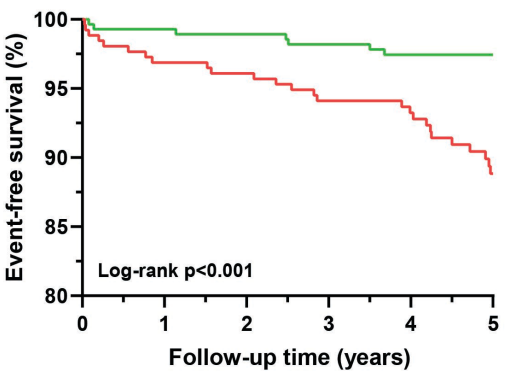

Non-ischemic	280	278	275	270	249	213
Ischemic	259	247	245	239	212	162

RCA PCATa

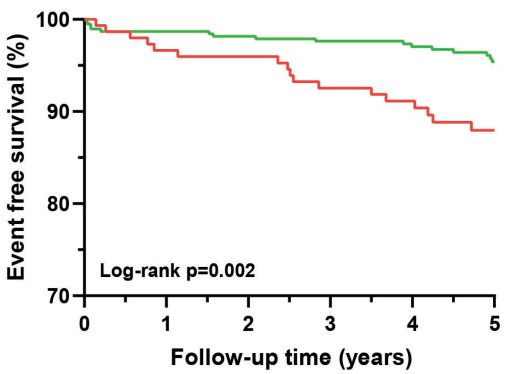

383	374	372	366	330	278	Below scanner specific threshold
149	144	142	137	125	92	Above scanner specific threshold